Sodium–calcium exchange does not require allosteric calcium activation at high cytosolic sodium concentrations

Jason Urbanczyk, Olga Chernysh, Madalina Condrescu and John P. Reeves

Department of Pharmacology and Physiology, University of Medicine and Dentistry of New Jersey, Graduate School of Biomedical Sciences, 185 South Orange Avenue, Newark, NJ 07101-1709, USA

The activity of the cardiac Na^+–Ca^{2+} exchanger (NCX1.1) is allosterically regulated by Ca^{2+}, which binds to two acidic regions in the cytosolically disposed central hydrophilic domain of the NCX protein. A mutation in one of the regulatory Ca^{2+} binding regions (D447V) increases the half-activation constant (K_h) for allosteric Ca^{2+} activation from ∼0.3 to $>1.8\,\mu$M. Chinese hamster ovary cells expressing the D447V exchanger showed little or no activity under physiological ionic conditions unless cytosolic [Ca^{2+}] was elevated to $>1\,\mu$M. However, when cytosolic [Na^+] was increased to 20 mM or more (using ouabain-induced inhibition of the Na^+,K^+-ATPase or the ionophore gramicidin), cells expressing the D447V mutant rapidly accumulated Ca^{2+} or Ba^{2+} when the reverse (Ca^{2+} influx) mode of NCX activity was initiated, although initial cytosolic [Ca^{2+}] was <100 nM. Importantly, the time course of Ca^{2+} uptake did not display the lag phase that reflects allosteric Ca^{2+} activation of NCX activity in the wild-type NCX1.1; indeed, at elevated [Na^+], the D447V mutant behaved similarly to the constitutively active deletion mutant Δ(241–680), which lacks the regulatory Ca^{2+} binding sites. In cells expressing wild-type NCX1.1, increasing concentrations of cytosolic Na^+ led to a progressive shortening of the lag phase for Ca^{2+} uptake. The effects of elevated [Na^+] developed rapidly and were fully reversible. The activity of the D447V mutant was markedly inhibited when phosphatidylinositol 4,5-bisphosphate (PIP2) levels were reduced. We conclude that when PIP2 levels are high, elevated cytosolic [Na^+] induces a mode of exchange activity that does not require allosteric Ca^{2+} activation.

(Resubmitted 19 May 2006; accepted after revision 23 June 2006; first published online 29 June 2006)
Corresponding author J. P. Reeves: Department of Pharmacology & Physiology, UMDNJ – NJ Medical School, 185 South Orange Avenue, PO Box 1709, Newark, NJ 07101-1709, USA. Email: reeves@umdnj.edu

The activity of the cardiac Na^+–Ca^{2+} exchanger (NCX1.1) is allosterically regulated by cytosolic Ca^{2+}, which appears to be required for all modes of NCX operation (DiPolo, 1979; Blaustein & Lederer, 1999). The regulatory Ca^{2+} binding sites are located in two acidic segments of the central hydrophilic domain (loop f) of the NCX protein (Levitsky *et al.* 1994; Matsuoka *et al.* 1995). The half-activation constant (K_h) for the allosteric Ca^{2+} activation is 200–600 nM in excised patches from cardiac myocytes or *Xenopus* oocytes expressing NCX1.1 (Hilgemann *et al.* 1992; Matsuoka *et al.* 1995, 1997), ∼300 nM in transfected Chinese hamster ovary (CHO) cells (Reeves & Condrescu, 2003), and 150 nM in guinea-pig ventricular cells (Weber *et al.* 2005); earlier reports had suggested much lower values (25–50 nM) in cardiac myocytes (Noda *et al.* 1988; Miura & Kimura, 1989) and transfected CHO cells (Fang *et al.* 1998). Ottolia *et al.* (2004) measured the affinity of the regulatory Ca^{2+} binding domain using a fusion protein designed to detect fluorescence resonance energy transfer (FRET) between donor and acceptor fluorescent proteins linked by the NCX regulatory Ca^{2+} binding domain. They determined the K_D to be 140 nM in the absence of Mg^{2+} and 383 nM in the presence of 1 mM Mg^{2+}; the latter value is more relevant to physiological cytosolic conditions.

Many recent studies of NCX regulation have been based on measurements of exchange currents in excised patches. These studies uniformly show that there is a strong requirement for allosteric Ca^{2+} activation for outward exchange currents elicited by high cytosolic Na^+ concentrations (typically 100 mM). Treating the patches with ATP, which induces the synthesis of phosphatidylinositol 4,5-bisphosphate (PIP2; Hilgemann & Ball, 1996), reduces the K_h for allosteric Ca^{2+} activation, and in some cases eliminates the need for allosteric Ca^{2+} activation (Collins *et al.* 1992); these effects are mimicked by the direct application of PIP2 to the patches (D. Hilgemann, personal communication). Here we report that in intact cells, exchange activity is observed at high cytosolic Na^+ concentrations ($[Na^+]_i$) in the absence of

 DOI: 10.1113/jphysiol.2006.113910

allosteric Ca^{2+} activation. We suggest that the difference between the behaviour of intact cells and excised patches reflects a higher membrane PIP2 content in intact cells. Our conclusions stem from measurements of exchange activity in transfected cells expressing a mutant exchanger that would be expected to show little or no allosteric Ca^{2+} activation at low cytosolic Ca^{2+} concentrations ($[Ca^{2+}]_i$).

Mutation of the acidic residues within the regulatory Ca^{2+} binding sites leads to an increase in the K_h for allosteric Ca^{2+} activation. Matsuoka *et al.* (1995) described one such mutant, D447V, which exhibited an apparent K_h of 1.8 μM. These investigators pointed out that the true K_h might be substantially higher because the increased cytosolic Ca^{2+} concentrations required for activation of the mutant competed with Na^+ at the translocation sites, causing a premature saturation of outward exchange currents. The FRET measurements of Ottolia *et al.* (2004) yielded a biphasic binding curve for the D447V mutant with K_D values of 1.2 and 2.5 μM in the absence of Mg^{2+}; K_D values in the presence of Mg^{2+} were not determined but would presumably be shifted to higher values.

In this report, we characterize the behaviour of the D447V mutant when expressed in CHO cells. We found that under normal physiological conditions, the exchanger showed little or no activity unless $[Ca^{2+}]_i$ was elevated to > 1 μM, consistent with the low affinity of the regulatory Ca^{2+} binding sites. However, when the cytosolic Na^+ concentration ($[Na^+]_i$) was elevated to 20 mM or more, cells expressing the D447V mutant rapidly accumulated Ca^{2+} or Ba^{2+} when the reverse (Ca^{2+} influx) mode of NCX activity was activated; this occurred at $[Ca^{2+}]_i$ concentrations that were initially below 100 nM. At elevated $[Na^+]_i$, the cells expressing the D447V mutant behaved very similarly to cells expressing a deletion mutant, Δ(241–680), which lacks the regulatory Ca^{2+} binding sites and operates constitutively. We conclude that the elevated $[Na^+]_i$ induces a mode of exchange activity that does not require allosteric Ca^{2+} activation.

Methods

Cells

CHO T cells (Chinese hamster ovary K1 cells expressing the human insulin receptor (Langille *et al.* 1999), kindly provided by Dr Michael Czech, University of Massachusetts Medical Center, Worcester, MA, USA) were transfected with the mammalian expression vector pcDNA3 containing the coding sequence for the canine cardiac Na^+–Ca^{2+} exchanger or the D447V mutant of the canine exchanger. Complementary DNAs for the canine wild-type and D447V mutant were kindly provided by Drs Deborah Nicoll and Kenneth D. Philipson (UCLA). Cells expressing Na^+–Ca^{2+} exchange activity were selected using the ionomycin-treatment procedure Iwamoto *et al.* (1998). Cells expressing the constitutive Δ(241–680) deletion mutant of the bovine cardiac Na^+–Ca^{2+} exchanger were prepared similarly. In this mutant, a large part of the central regulatory domain of the exchanger has been deleted, including the regulatory Ca^{2+} binding sites. The Δ(241–680) mutant does not require allosteric activation by cytosolic Ca^{2+} for activity (Matsuoka *et al.* 1993); the behaviour of exchange activity in these cells has been described in several recent publications (Reeves & Condrescu, 2003; Chernysh *et al.* 2004; Condrescu & Reeves, 2006). In this report, we will refer to cells expressing the wild-type and mutant exchangers as wild-type, D447V and Δ(241–680) cells. All cells were grown in Hams' F-12 (modified) medium supplemented with 10% fetal bovine serum, 2 mM L-glutamine, 100 U ml^{-1} penicillin, 100 μg ml^{-1} streptomycin and 20 μg ml^{-1} gentamicin.

Solutions

Sodium-physiological saline solution (Na-PSS) contained 140 mM NaCl, 5 mM KCl, 1 mM $MgCl_2$, 10 mM glucose and 20 mM 3-(*N*-morpholino)propanesulphonic acid (Mops), buffered to pH 7.4 with Tris. The composition of K-PSS was similar except that NaCl was absent and the total concentration of KCl was 140 mM. Solutions designated 5/140, 10/130, 20/120, 40/100, etc. Na/K-PSS contained the indicated concentrations of Na^+ and K^+ (e.g. 5 mM NaCl + 140 mM KCl) plus 1 mM $MgCl_2$, 10 mM glucose and 20 mM Mops/Tris, pH 7.4. Biochemicals were purchased from Sigma, unless indicated otherwise, and cell culture media, including fetal bovine serum, were from Life Technologies.

Fura-2 imaging

Cells were grown on 25 mm circular coverslips and loaded with fura-2 by incubating the coverslips for 30–40 min at room temperature in Na-PSS containing 1 mM $CaCl_2$, 1% bovine serum albumin, 0.25 mM sulphinpyrazone (to retard fura-2 transport from the cell) and 3 μM fura-2 AM (Molecular Probes). The coverslips were then washed in Na-PSS + 1 mM $CaCl_2$, placed in a stainless-steel holder (bath volume, ~0.8 ml; Molecular Probes), and viewed in a Zeiss Axiovert 100 microscope coupled to an Attofluor digital imaging system. Forty to 60 individual cells were selected and monitored simultaneously for each coverslip. Results are presented as the ratio (R) of fluorescence intensities, after correction for background emission (see below), at excitation wavelengths of 334 nm (350 nm for Ba^{2+}) and 380 nm (390 nm for Ba^{2+}) or, after calibration, as the cytosolic Ca^{2+} concentration. Emission was monitored at > 510 nm. Calibrations utilized the relation of Grynkiewicz *et al.* (1985):

$$[Ca^{2+}]_i = K_{D,fura}(Sf/Sb)(R - R_{min})/(R_{max} - R)$$

where Sf/Sb, R_{min}, R_{max} and R were determined for individual cells as described by Reeves & Condrescu (2003). Background fluorescence was determined at the end of each experiment by applying 10 mM $MnCl_2$ in the presence of 1 or 10 μM ionomycin to quench fura-2 fluorescence. Background fluorescence was subtracted from all fluorescence values and ratios were recalculated to yield R, R_{min} and R_{max}; Sf/Sb is the ratio of corrected fluorescence intensities at 380 nm under conditions for determination of R_{min} (Sf) and R_{max} (Sb). The K_D for fura-2 was assumed to be 224 nM (Grynkiewicz *et al.* 1985). Maximal rates of Ca^{2+} uptake were determined as previously described (Reeves & Condrescu, 2003). Briefly, the rate of change in the fura-2 ratio was determined for each cell by evaluating the slope over a rolling four-data-point interval throughout the time course of Ca^{2+} uptake. The maximal slopes were identified by spreadsheet analysis and, for each coverslip, the average maximal slope of all the cells was computed. Results are presented as the mean (± S.E.M.) for the indicated number of coverslips.

Measurement of NCX activity

Most experiments used the monovalent cation channel-forming ionophore gramicidin to clamp cytosolic $[Na^+]$ at the desired level. Unless otherwise specified, Ca^{2+} was released from the endoplasmic reticulum approximately 10 min before beginning the recordings by applying 100 μM ATP and 2 μM thapsigargin (Tg), an irreversible and selective inhibitor of the sarco(endo)plasmic reticulum Ca^{2+}-ATPase (Lytton *et al.* 1991), in Na-PSS + 0.3 mM EGTA. Approximately 8 min before beginning the recordings, the coverslip was washed with 5 ml of the desired Na/K-PSS solution containing 0.3 mM EGTA, and 1 ml of the same solution containing 1 μg ml^{-1} gramicidin was then added. To initiate the Ca^{2+} influx ('reverse') mode of NCX activity, 0.1 mM $CaCl_2$ in the Na/K-PSS solution used for the pre-incubation with gramicidin was manually applied to the cells using a syringe with continuous aspiration of excess solution. In some experiments, gramicidin was omitted and the cells were pre-incubated in Na-PSS + 0.3 mM EGTA under the conditions specified for the individual experiments; in this case, Na^+–Ca^{2+} exchange activity was initiated by applying 0.1 mM $CaCl_2$ in K-PSS. Experiments were carried out at 37°C unless otherwise specified. Each experiment shown was repeated at least four times with similar results.

For the experiment shown in Fig. 1, mixtures of transfected and non-transfected CHO cells were grown on the same coverslip. After completion of the experiment, the two cell types were identified by applying Na-PSS containing 1 μg ml^{-1} gramicidin and, 3–4 min later, initiating reverse exchange activity by applying 0.1 mM $CaCl_2$ in K-PSS. Under these conditions, only cells expressing NCX activity accumulated Ca^{2+} (Chernysh *et al.* 2004).

Rhod-2 measurements

For experiments in which rhod-2 was used to measure mitochondrial Ca^{2+} uptake, the cells were loaded with fura-2 for 40 min as described above. This was necessary in order to keep the cytosolic Ca^{2+} buffering approximately the same as in the fura-2 experiments. Rhod-2 AM (2 μM) was added to the loading medium for the final 10–12 min of incubation. Rhod-2 fluorescence was monitored at 520–560 nm after excitation at 488 nm following the general procedures previously described (Opuni & Reeves, 2000).

Imaging cellular PIP2

Várnai *et al.* (2002) described the use of a fusion protein linking green fluorescent protein (GFP) with the pleckstrin homology (PH) domain of phospholipase Cδ1 (PLCδ1PH-GFP) to visualize cellular levels of PIP2. The PH domain of PLCδ1PH-GFP binds strongly to PIP2. Under normal conditions, the probe was localized primarily to the plasma membrane, but when PIP2 levels were reduced (e.g. by elevating $[Ca^{2+}]_i$ with ionomycin), the PLCδ1PH-GFP moved from the membrane to the cytoplasm and a more diffuse distribution was observed (Várnai *et al.* 2002). D447V cells were transfected (lipofectamine) with cDNA for PLCδ1PH-GFP, kindly provided by Dr Tamas Balla (NICHD, NIH) through Dr Larry Gaspers (UMDNJ), and 48 h later were visualized using a Zeiss Axiovert 100 fluorescence microscope equipped with a Zeiss AxioCam digital camera. Excitation was at 488 nm and emission was observed at 535 nm using appropriate filters.

Results

Ca^{2+} efflux activity of the D447V mutant

The D447V mutant was well expressed in CHO cells, as determined from immunofluorescence images (data not shown); it was highly concentrated in the plasma membrane and its distribution was indistinguishable from that of the wild-type NCX, as recently described (Condrescu & Reeves, 2006).

Transfected CHO cells expressing the D447V mutant of the canine cardiac NCX1.1 were grown on coverslips along with non-transfected CHO cells. The cells were loaded with fura-2 and, in the experiment shown in Fig. 1, 100 μM ATP and 2 μM thapsigargin (Tg) were added to elicit the release of Ca^{2+} from the endoplasmic reticulum

(ER). At the end of this experiment, the transfected and non-transfected cells were identified by assaying for NCX activity as described in the Methods. The amplitudes and durations of the resulting $[Ca^{2+}]_i$ transients were practically identical in both types of cells, suggesting that Ca^{2+} efflux activity by D447V was minimal under these conditions. The fura-2 ratios in this experiment were not calibrated, but previous studies (Chernysh *et al.* 2004) have shown that $[Ca^{2+}]_i$ rises to several micromolar at the peak of the $[Ca^{2+}]_i$ transient.

Since mitochondria accumulate substantial quantities of Ca^{2+} at high values of $[Ca^{2+}]_i$, we were concerned that mitochondrial Ca^{2+} uptake might influence the results. This concern was well founded, as shown by the results in Fig. 1*B*. Here, ER Ca^{2+} was released with ATP and Tg in the presence of carbonyl cyanide *m*-chlorophenylhydrazone (Cl-CCP; 5 μM), a mitochondrial uncoupler, and oligomycin (1 μg ml^{-1}), an inhibitor of the F_oF_1-ATPase. Under these conditions, the Ca^{2+} transient of the non-transfected cells was increased in magnitude and duration while that for the cells expressing D447V was not greatly affected. Thus, in the presence of Cl-CCP, the $[Ca^{2+}]_i$ transient was attenuated in the cells expressing the D447V mutant compared to the non-transfected CHO cells. Figure 1*C* shows an experiment identical to that in Fig. 1*B* except that cells expressing the wild-type exchanger were used; in this case, the $[Ca^{2+}]_i$ transient of the NCX-expressing cells was greatly reduced compared to that seen with the cells expressing D447V.

The reduced size of the $[Ca^{2+}]_i$ transients in cells expressing the wild-type or mutant NCX could reflect either NCX-mediated Ca^{2+} efflux or different amounts of releasable Ca^{2+}. The latter possibilitiy was ruled out by experiments in which ATP and Tg were applied (in the presence of Cl-CCP) in a Na^+-free medium (K-PSS) so that the exchanger would not contribute to Ca^{2+} efflux. As shown in Fig. 1*D*, the $[Ca^{2+}]_i$ transient displayed by the cells expressing D447V was prolonged in comparison to that seen in the presence of Na^+ and was essentially identical to that shown by the non-transfected cells. In cells expressing the wild-type exchanger, the amplitude of the $[Ca^{2+}]_i$ transient in K-PSS was also essentially identical to that shown by the non-transfected cells (data not shown). We conclude that NCX-mediated Ca^{2+} efflux is responsible for the reduced amplitude of the $[Ca^{2+}]_i$ transients in cells expressing D447V or wild-type NCX compared to non-transfected cells (Fig. 1*B* and *C*).

It is striking that Ca^{2+} efflux by D447V was not apparent at high $[Ca^{2+}]_i$ unless Cl-CCP was added to prevent mitochondrial Ca^{2+} uptake (Fig. 1). The simplest explanation for this behaviour is that, in the absence of Cl-CCP, Ca^{2+} efflux activity of the partly activated D447V exchanger diverted some of the Ca^{2+} that would otherwise be accumulated by mitochondria, yielding a fortuitous similarity in the amplitude of the $[Ca^{2+}]_i$ transients. This hypothesis is supported by the data in Fig. 1*E*, in which cells expressing D447V and non-transfected CHO cells were loaded with the mitochondrial Ca^{2+} probe rhod-2 to examine changes in

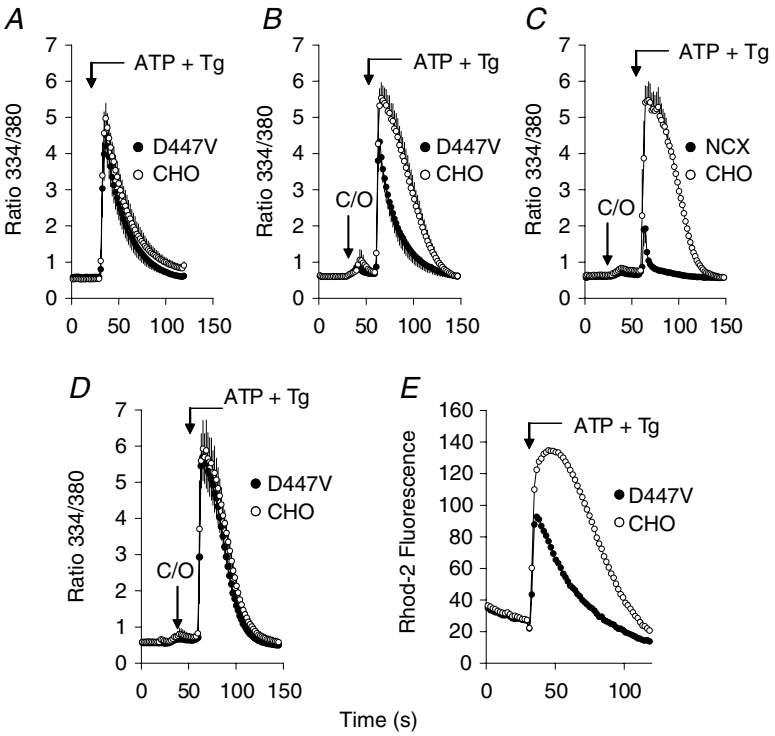

Figure 1. Ca^{2+} efflux in cells expressing the D447V mutant
Non-transfected CHO cells and cells expressing the D447V mutant (*A*, *B*, *D* and *E*) or wild-type canine exchanger (*C*) were grown together on the same coverslip and loaded with fura-2. Immediately before beginning the recordings, the coverslips were washed with Na-PSS containing 0.3 mM EGTA (Na-PSS/EGTA). *A*, ATP (100 μM) and Tg (2 μM) in Na-PSS/EGTA were applied to release Ca^{2+} from the ER ($n = 6$ coverslips; vertical bars denote S.E.M.). *B*, as in *A* except that 1 ml of Na-PSS/EGTA containing 5 μM Cl-CCP and 1 μg ml^{-1} oligomycin (arrow labelled C/O) was applied 30 s prior to adding ATP and Tg in Na-PSS/EGTA containing 5 μM Cl-CCP ($n = 5$). *C*, as in *B* except that the experiment was carried out with cells expressing the wild-type NCX1.1 instead of the D447V mutant ($n = 3$). *D*, as in *B* except that the experiment was carried out in a Na^+-free medium (K-PSS; $n = 4$). *E*, cells were loaded with rhod-2 as described in the Methods. Application of ATP and Tg was in Na-PSS/EGTA, and mitochondrial Ca^{2+} uptake was monitored as an increase rhod-2 fluorescence.

mitochondrial Ca^{2+} in the types of experiments described above. Both types of cells showed mitochondrial Ca^{2+} accumulation following the application of ATP and Tg, but Ca^{2+} uptake was reduced in amplitude and decayed more quickly in the cells expressing D447V. This undoubtedly resulted from Ca^{2+} efflux mediated by D447V; indeed, when the experiment was repeated in the absence of extracellular Na^+ (K-PSS), mitochondrial Ca^{2+} uptake in the two types of cells was essentially the same (data not shown).

Ca^{2+} influx mode of NCX activity

We incubated cells expressing the D447V mutant for 10 min at 37°C in Na-PSS/EGTA with or without 1 mM ouabain, an inhibitor of the Na^+,K^+-ATPase. In the absence of ouabain, as shown in Fig. 2*A* (○), cells expressing D447V displayed practically no Ca^{2+} uptake when reverse exchange activity was initiated by applying 0.1 mM $CaCl_2$ in K-PSS. Since the initial $[Ca^{2+}]_i$ in these experiments was 25 nM, the exchanger was undoubtedly inactive because of the absence of allosteric Ca^{2+} activation. However, after 10 min with 1 mM ouabain, conditions that would lead to an elevation in the cytosolic Na^+ concentration, the cells accumulated Ca^{2+} when reverse-mode exchange activity was initiated, even though the intitial $[Ca^{2+}]_i$ was the same as in the absence of ouabain (Fig. 2*A*, ●). Figure 2*B* shows the behaviour of several of the individual D447V-expressing cells in this experiment. For each of the cells, Ca^{2+} uptake began immediately after the solution change and continued in a nearly linear fashion until a peak value of $[Ca^{2+}]_i$ was approached.

To be sure that ouabain had not induced a Ca^{2+} entry pathway other than Na^+–Ca^{2+} exchange activity, we repeated this experiment, this time with 15 min of ouabain treatment, using coverslips containing both non-transfected and D447V-expressing cells. As shown in Fig. 2*C*, Ca^{2+} uptake by the non-transfected CHO cells was very small in comparison to that by the cells expressing D447V. In this experiment, Ca^{2+} uptake by the D447V cells was much greater than for the experiment in Fig. 2*A*, presumably because of the increased incubation time with ouabain. Thus, ouabain acts by stimulating NCX activity in the cells expressing D447V.

Since the initial $[Ca^{2+}]_i$ (25 nM) was very far below the K_h for allosteric Ca^{2+} activation of the D446V mutant, we had expected to see little or no Ca^{2+} uptake in the ouabain-treated cells even though cytosolic Na^+ concentrations were elevated. To further investigate the influence of cytosolic Na^+, we carried out the experiments described below, in which we used gramicidin, a monovalent cation channel-forming ionophore, to clamp $[Na^+]_i$ at specified values.

Na^+ concentration dependence

In Fig. 3*A*, cells expressing the D447V mutant were treated with gramicidin (1 μg ml^{-1}) to permeabilize the plasma membrane to monovalent cations and loaded with Na^+

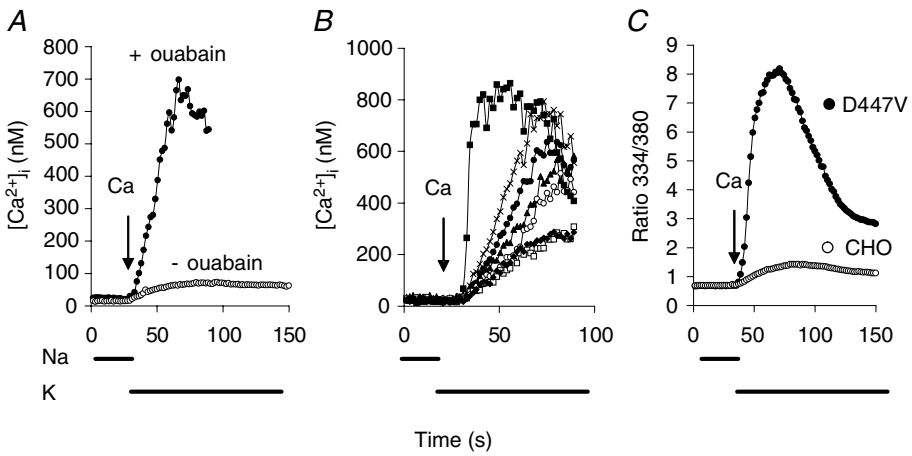

Figure 2. Ca^{2+} uptake in ouabain-treated cells
A, 10 min before beginning recordings, cells were treated with ATP and Tg in Na-PSS/EGTA with (●) or without 1 mM ouabain (○). Activity of NCX was initiated by applying 0.1 mM $CaCl_2$ in K-PSS as indicated. The traces represent the average responses of 60 cells from single coverslips. *B*, traces from several of the individual ouabain-treated cells from the experiment shown in *A*. *C*, coverslips containing a mixture of D447V and non-transfected CHO cells were treated with ATP and Tg in Na-PSS/EGTA for 15 min before beginning recordings. Activity of NCX was initiated by applying 0.1 mM $CaCl_2$ in K-PSS as indicated. The peak ratio in this experiment (~8) was much higher than the peak ratio observed for the experiment in *A* (~2), most probably because of the increased incubation time with ouabain. The trace represents the average response of 44 D447V cells and 20 CHO cells from a single cover slip.

concentrations ranging from 10 to 140 mM. The cells were then assayed for Ba^{2+} uptake in K-PSS containing 1 mM $BaCl_2$; previous studies have shown that Ba^{2+} uptake under these conditions is due solely to reverse NCX activity (Condrescu *et al.* 1997). As shown, little or no Ba^{2+} uptake was observed after loading with 10 or 20 mM Na^+ (these traces overlap in Fig. 3*A*), but a progressive increase in the rate and extent of Ba^{2+} uptake was seen at higher Na^+ concentrations. Calibrations were not conducted in these experiments, but the initial $[Ca^{2+}]_i$ before the addition of Ba^{2+} was undoubtedly similar to that shown in Fig. 2, i.e. < 100 nM. In view of the low affinity of the allosteric Ca^{2+} binding sites of the mutant exchanger, it is remarkable that Ba^{2+} uptake was observed at any Na^+ concentration. Although Ba^{2+} is able to substitute for Ca^{2+} at the wild-type allosteric activation sites, the affinity of these sites for Ba^{2+} is much less than for Ca^{2+} (10 *versus* 0.3 μM; Trac *et al.* 1997); thus, it is extremely unlikely that Ba^{2+} itself could be activating the mutant in these experiments. The results suggest that the requirement for allosteric Ca^{2+} activation is reduced or eliminated at high concentrations of cytosolic Na^+.

The data in Fig. 3*B* show Ca^{2+} uptake by gramicidin-treated cells expressing the D447V mutant after equilibration with 5, 10, 20 and 40 mM Na^+. In this experiment, reverse NCX activity was initiated by applying 0.1 mM Ca^{2+} in Na/K-PSS solutions containing the same Na^+ concentrations as in the pre-equilibration medium. Little or no Ca^{2+} uptake was observed at 5 mM Na^+, slightly more at 10 mM Na^+, and higher rates of Ca^{2+} uptake were seen with 20 and 40 mM Na^+. We conclude that Na^+ concentrations in excess of 5 mM progressively activate the mutant exchanger at initial cytosolic Ca^{2+} concentrations < 100 nM.

Figure 3*C* and *D* shows the results of identical experiments carried out with either the wild-type exchanger or a mutant, Δ(241–680), in which the allosteric Ca^{2+} binding sites have been deleted so that exchange activity operates in the absence of allosteric Ca^{2+} activation. At 5 mM Na^+, wild-type cells showed a pronounced delay (lag period) before significant amounts of Ca^{2+} were taken up (Fig. 3*C*). We described this behaviour in detail in a previous publication (Reeves & Condrescu, 2003). Briefly, the lag period reflects the absence of significant allosteric Ca^{2+} activation at the low initial values of $[Ca^{2+}]_i$; as Ca^{2+} uptake slowly progresses, the exchangers become increasingly activated and Ca^{2+} uptake accelerates by positive feedback. At higher $[Na^+]$, the lag periods were progressively shortened and the rates of Ca^{2+} uptake increased. In contrast, as shown in Fig. 3*D*, no lag was observed at any Na^+ concentration for cells expressing the Δ(241–680) mutant, as previously described (Reeves & Condrescu, 2003). Although the rate and extent of Ca^{2+} uptake was lower at 5 mM than at

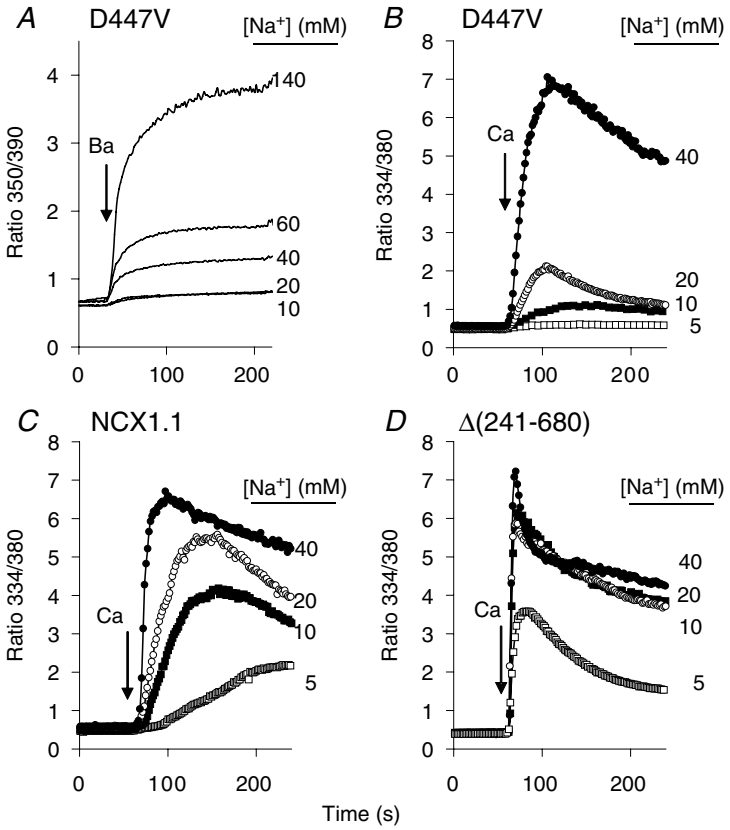

Figure 3. Ca^{2+} and Ba^{2+} uptake in gramicidin-treated cells
Cells expressing the D447V mutant were treated with ATP and Tg in Na-PSS/EGTA 10 min before beginning the recordings. All traces represent the average response of > 50 cells from single coverslips. *A*, 3 min before beginning recordings, the cells were treated with 1 μg ml^{-1} gramicidin in Na/K-PSS solutions containing the Na^+ concentrations indicated in the figure. Barium uptake was initiated by applying K-PSS containing 1 mM $BaCl_2$ and 0.1 mM EGTA (the latter was included to chelate residual Ca^{2+}). *B*, D447V cells were treated with ATP, Tg and gramicidin in Na/K-PSS solutions containing 5, 10, 20 and 40 mM Na^+; in these experiments, gramicidin was applied 8 min before beginning the recordings. Reverse NCX activity was initiated by applying 0.1 mM $CaCl_2$ in the same Na/K-PSS solution used for the pre-incubation (arrow labelled 'Ca'). *C*, the procedure was the same as described for *B*, except that cells expressing the wild-type NCX1.1 were used. *D*, as in *B*, except that Δ(241–680) cells were used.

the higher Na^+ concentrations, the traces at the higher concentrations were indistinguishable.

Figure 4 displays traces for several individual cells from the experiments at 20 mM Na^+ in Fig. 3. D447V cells (Fig. 4*A*) displayed Ca^{2+} uptake without a discernable lag period. There was considerable variability in the rate and extent of Ca^{2+} uptake among the individual cells, which probably reflects cellular variability in NCX expression. For many of the cells, Ca^{2+} uptake increased to a peak value and then declined; this behaviour is discussed in a later section of this report. In contrast to the cells expressing D447V, many of the wild-type cells (Fig. 4*B*) displayed lag periods of several tens of seconds; the average (± S.D.) time to attain maximal rates of Ca^{2+} uptake following the addition of Ca^{2+} was 38 ± 24 s for the 56 cells in this experiment. The lag periods for the wild-type cells were considerably longer at 10 and 5 mM Na^+ (data not shown). Cells expressing the Δ(241–680) mutant (Fig. 4*C*), showed very rapid uptake with no lag periods; essentially all the cells behaved similarly and only three cells are shown in the figure to maintain clarity.

Maximal rates of Ca^{2+} uptake in 40/100 Na/K-PSS following the addition of 0.1 mM Ca^{2+} were computed for each coverslip as the average of the slopes of the fura-2 traces for the individual cells as described in the Methods. The mean value (± S.E.M.) for D447V cells was 0.68 ± 0.07 ratio units s^{-1} (n = 9 coverslips). The corresponding values for wild-type and Δ(241–680) cells were 1.32 ± 0.23 (n = 5) and 1.17 ± 0.07 ratio units s^{-1} (n = 7), respectively ($P < 0.01$ for both comparisons *versus* D447V; Student's t test). Thus, at 40 mM Na^+, exchange activity of the D447V cells was 40–50% lower than for either the wild-type or Δ(241–680) cells.

PIP2 and NCX activity of the D447V mutant

As mentioned previously, at 20 mM Na^+, a decline in $[Ca^{2+}]_i$ following the peak value was observed for many of the cells expressing D447V (Fig. 4*A*). The decline did not result from a decrease in $[Na^+]_i$, since gramicidin clamped $[Na^+]_i$ at 20 mM in this experiment. Part of the decline can be attributed to mitochondrial Ca^{2+} uptake, as shown by the results in Fig. 5*A*. In these experiments, gramicidin-treated D447V cells were equilibrated with 20/120 Na/K-PSS and then treated with either DMSO (●) or with oligomycin and Cl-CCP (○) to block mitochondrial Ca^{2+} uptake. NCX activity was initiated by applying 0.1 mM Ca^{2+} in 20/120 Na/K-PSS with or without 5 μM Cl-CCP, as indicated. The rise in $[Ca^{2+}]_i$ was much greater in the presence of Cl-CCP than in its absence and did not show a postpeak decline. Ca^{2+} uptake was terminated after 3 min by applying 0.3 mM EGTA and, after an additional 60 s, a second round of Ca^{2+} uptake was initiated. In all solutions for the traces with the open circles, Cl-CCP was present. Calcium uptake was reduced during the second application of Ca^{2+} compared to the first, suggesting that the exchanger had lost activity during the first interval of Ca^{2+} uptake. It appears that the combination of NCX inactivation and mitochondrial Ca^{2+} accumulation is responsible for the postpeak decline in $[Ca^{2+}]_i$ noted earlier.

Additional experiments were conducted to characterize the inactivation process further; these were carried out at room temperature to slow the recovery of exchange activity following the termination of Ca^{2+} influx. The results, taken together with the data in Fig. 6, provide strong evidence that the inhibition of D447V activity following the initial period of Ca^{2+} uptake results from a decline in PIP2. For the data in Fig. 5*B*, D447V cells were pretreated with gramicidin in 40/100 Na/K-PSS. Reverse NCX activity was then induced by applying 0.1 mM Ca^{2+} in 40/100 Na/K-PSS containing the mitochondrial uncoupler Cl-CCP. Calcium uptake was terminated after 60 s by applying EGTA and, after $[Ca^{2+}]_i$ had returned to its initial value, 0.1 mM Ca^{2+} was applied a second time. As shown in Fig. 5*B*, practically no Ca^{2+} uptake was observed during the second Ca^{2+} application (at 200 s), indicating a profound inhibition of NCX activity following the initial increase in $[Ca^{2+}]_i$. If extracellular Ca^{2+} was then removed for an interval of several minutes, a third application of 0.1 mM Ca^{2+}

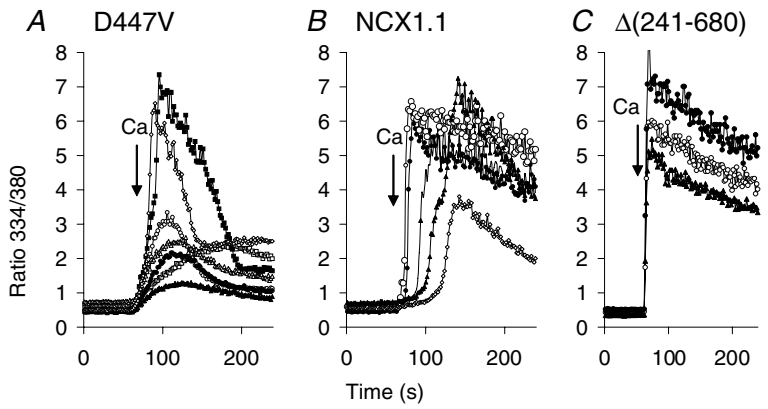

Figure 4. Ca^{2+} uptake by individual D447V, NCX1.1 or Δ(241–680) cells
Traces for several of the individual cells from the coverslips used for the experiment in 20/120 Na/K-PSS from Fig. 3. *A*, D447V cells; *B*, NCX1.1 cells; and *C*, Δ(241–680) cells.

(at 630 s) showed that NCX activity had recovered. In these experiments, Cl-CCP was included during the initial period of Ca^{2+} uptake, but not in the subsequent solutions; essentially identical results were obtained if Cl-CCP was included in all solutions (data not shown).

When this experiment was repeated with cells expressing the Δ(241–680) mutant, rapid rates of Ca^{2+} uptake were seen shortly after the initial response was terminated (Fig. 5*C*). Thus, the activity of the Δ(241–680) mutant was unaffected by the prior elevation of $[Ca^{2+}]_i$. Cells expressing the wild-type exchanger (Fig. 5*D*) behaved very similarly to the Δ(241–680) cells, i.e. rapid Ca^{2+} uptake was observed upon initiation of NCX activity following the decay of the first Ca^{2+} transient. This probably reflects the persistence of allosteric Ca^{2+} activation of the exchanger following the initial period of Ca^{2+} uptake (Reeves & Condrescu, 2003), and implies that allosteric Ca^{2+} activation overrides the process leading to inactivation of NCX during the first period of Ca^{2+} uptake.

Most isoforms of phospholipase C are activated by high concentrations of Ca^{2+}, although the PLC δ_1 isoform is more sensitive in this regard (Rhee, 2001; Balla, 2006). In CHO cells, the elevation of cytosolic Ca^{2+} with ionomycin induced a marked decline in PIP2 (Aharonovitz *et al.* 2000); this was assessed by the distribution of a fusion protein linking the plekstrin homology (PH) domain of the δ_1 isoform of PLC with green fluorescent protein (PLCδ_1PH-GFP; Varnai *et al.* 2002). The PH domain of PLCδ_1 binds tightly to PIP2; it localizes to the plasma membrane when PIP2 levels are high, but distributes throughout the cell when PIP2 levels fall (Várnai *et al.* 2002). We used this approach to determine the effects on PIP2 of Ca^{2+} influx mediated by reverse NCX activity.

Cells expressing D447V were loaded for 30 min with fura-2 to be certain that cytosolic Ca^{2+} buffering was comparable to the conditions in Fig. 5. We then treated the cells with gramicidin in 40/100 Na/K-PSS and initiated reverse NCX activity by applying 0.1 mM Ca^{2+} in the presence of Cl-CCP, following the same schedule of additions as in the experiments in Fig. 5*B*–*D*. Figure 6 shows images of the D447V cells expressing PLCδ_1PH-GFP at various time points during the experiment, along with the intensity profiles of the images, taken along the white line shown in the top image. Prior to the initiation of Ca^{2+} influx (labelled 'before' in Fig. 6) the PLCδ_1PH-GFP fusion protein was highly concentrated at the plasma membrane, as expected for cells with a normal complement of PIP2. Calcium influx was initiated at 60 s, and after an additional 60 s (120 s in the figure), the fusion protein was distributed throughout the cytosol, consistent with a sharp reduction of plasma membrane PIP2. Following removal of extracellular Ca^{2+}, the initial distribution of the fusion protein was gradually restored. At 195 s, corresponding to the approximate time of the second Ca^{2+} addition

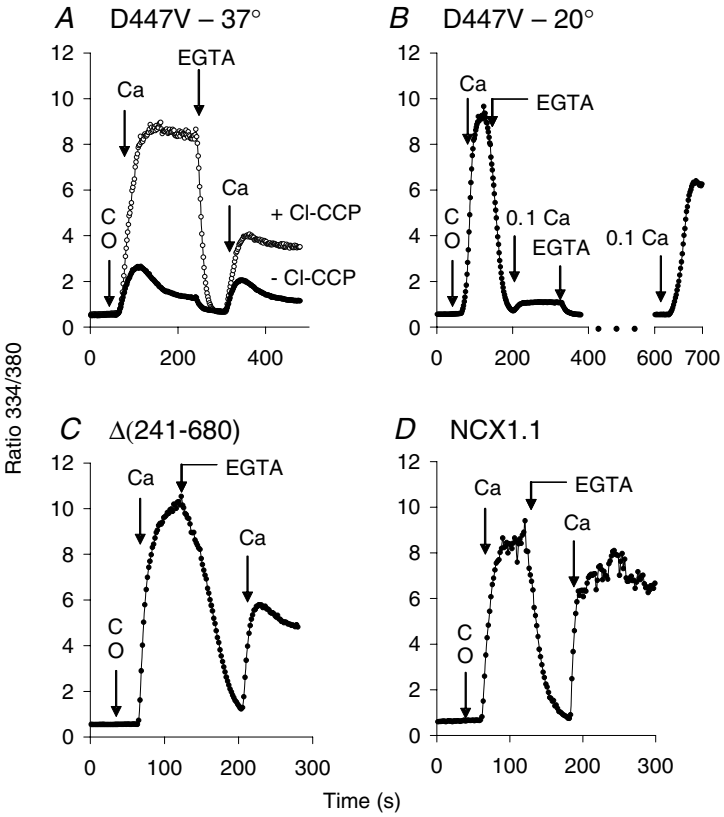

Figure 5. Effect of elevated $[Ca^{2+}]_i$ on NCX activity of cells expressing D447V
All traces reflect the average response of > 50 cells from single coverslips. *A*, cells expressing D447V were treated with ATP/Tg in Na-PSS/EGTA, and with gramicidin in 20/120 Na/K-PSS/EGTA, 10 and 8 min, respectively, before beginning recordings. At $t = 30$ s, 1 ml of 20/120 Na/K-PSS containing 0.2% DMSO or 5 μM Cl-CCP plus 1 μg ml^{-1} oligomycin was applied, as indicated by the arrow labelled 'CO'. Four millilitres of 0.1 mM $CaCl_2$ in 20/120 Na/K-PSS with 0.1% DMSO or 5 μM Cl-CCP were applied at 60 s, 20/120 Na/K-PSS with 0.1% DMSO or 5 μM Cl-CCP was applied at 240 s, and 0.1 mM $CaCl_2$ with 0.1% DMSO or 5 μM Cl-CCP was re-applied at 300 s. *B*, the general protocol was similar to that for the Cl-CCP-treated cells in *A*. In this case, however, the experiment was run at room temperature rather than 37°C, 40/100 Na/K-PSS was used instead of 20/120 Na/K-PSS, and Cl-CCP was omitted from all solutions applied after 60 s. At 330 s, 40/100 Na/K-PSS and 0.3 mM EGTA was applied, and at 630 s, 0.1 mM $CaCl_2$ in 40/100 Na/K-PSS was again applied. *C*, the general protocol was similar to that described for *B*, except that cells expressing the Δ(241–680) mutant were used. *D*, as in *B* and *C* except that cells expressing the wild-type NCX1.1 were used.

in Fig. 5*B*, the PLCδ_1PH-GFP had started to return to the plasma membrane, although considerable cytoplasmic fluorescence was still observed. By 300 s, initial conditions were nearly restored. These results suggest that the decline in PIP2 during the first interval of Ca^{2+} uptake was responsible for the inhibition of exchange activity in the D447V mutant (Fig. 5*A* and *B*).

Time dependence of activation and reversal

It is important to know whether elevated cytosolic Na^+ activates NCX activity instantaneously or in a time-dependent manner. To examine this issue, we pre-equilibrated gramicidin-treated cells expressing D447V with a low concentration of Na^+ (5 mM); we then applied 40 mM Na/K-PSS and measured Ca^{2+} uptake at intervals after the solution switch. Figure 7*A* displays the data obtained when NCX activity was initiated 0.5, 1, 2 or 5 min following the transfer to 40 mM Na^+; also shown (▲) is a trace for Ca^{2+} uptake in 5 mM Na^+. The various traces are superimposed in Fig. 7*B*. As shown, rapid rates of Ca^{2+} uptake were observed as early as 30 s after the solution change, indicating that elevated Na^+ stimulates activity very rapidly. Longer periods at 40 mM Na^+ did not induce higher levels of activity.

To determine whether the effects of elevated cytosolic [Na^+] were reversible, we carried out the inverse of the experiments in Fig. 7*A*. As shown in Fig. 7*C*, cells expressing the D447V mutant were pre-equilibrated with 40/100 Na/K-PSS in the presence of gramicidin and

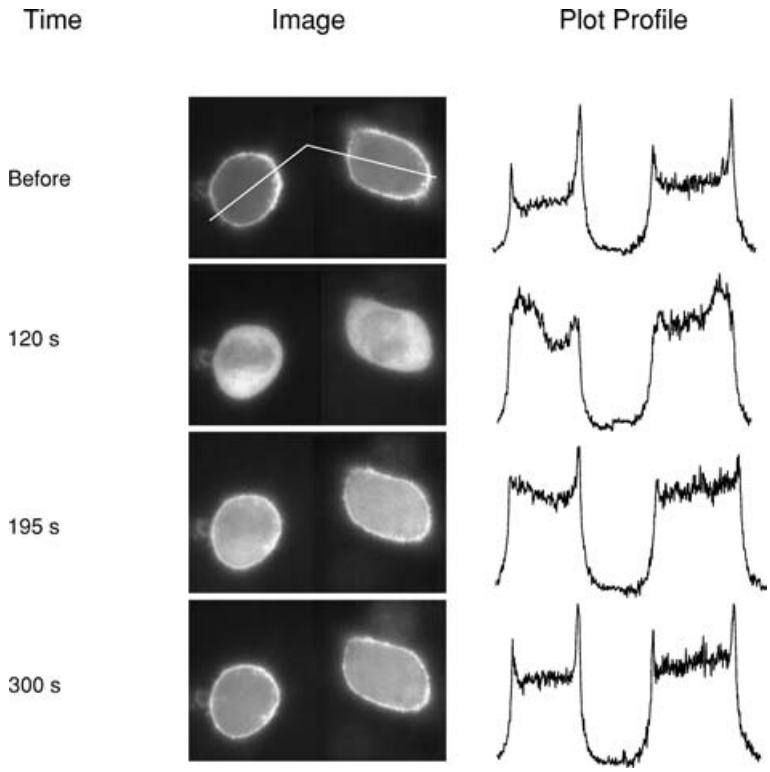

Figure 6. Changes in PIP2 associated with elevated $[Ca^{2+}]_i$
Cells expressing the D447V mutant were transfected with cDNA coding for PLCδ1PH-GFP. Forty-eight hours later, the distribution of PLCδ1PH-GFP was monitored during the solution changes described in Fig. 5. The cells were loaded with fura-2 to ensure that cytosolic Ca^{2+} buffering was equivalent to the experiments in Fig. 5*B*. The cells were then treated with ATP and Tg, with gramicidin in 40/100 Na/K-PSS, and the procedure described in the legend to Fig. 5*B* was followed, i.e. Cl-CCP and oligomycin were added at 30 s, 0.1 mM Ca^{2+} and Cl-CCP were applied at 60 s, and 0.3 mM EGTA was applied at approximately 120 s; the experiment was conducted at room temperature. The times given in the left column correspond to the time axis in Fig. 5*B*, i.e. the image labelled 'Before' was taken prior to the initiation of the experiment, the image at 120 s was taken just prior to the application of 0.3 mM EGTA, and images were subsequently taken at 195 and 300 s. A second application of Ca^{2+} (e.g. at 200 s) was not done in this experiment; in other experiments, we found that the second application of Ca^{2+} reversed the recovery process so that fluorescence again became cytosolic. The two cells shown are from the same coverslip. However, since their fluorescence intensities were different, the brightness and contrast for each cell was independently adjusted using the auto feature of the Adobe Photoshop CS program. The traces on the right side of each image show the intensity profiles along the white lines depicted in the top image, as determined using the Image J program.

transferred to 5/140 Na/K-PSS; Ca^{2+} uptake was then measured at 0.5, 1, 2 and 5 min after the solution change. A control trace (Fig. 7*C*; ▲) is also shown in which Ca^{2+} uptake was measured in 40/100 Na/K-PSS without a solution change. The various traces in Fig. 7*C* are superimposed in Fig. 7*D*. Note that the rate of Ca^{2+} uptake declined markedly between 30 and 60 s after the solution change and was negligible after 5 min in 5/140 Na/K-PSS. We conclude that the effects of elevated Na^+ are fully reversible and cannot be attributed to some permanent change in the D447V protein (such as proteolysis) that might have been induced by the high $[Na^+]_i$.

Discussion

The use of the D447V mutant has revealed an unexpected relationship between $[Na^+]_i$ and allosteric Ca^{2+} activation of NCX, i.e. that activity becomes independent of allosteric Ca^{2+} activation at elevated $[Na^+]_i$ (constitutive NCX activity). For the D447V mutant, the high value for the K_h for allosteric Ca^{2+} activation ($> 1.8\,\mu$M; Matsuoka *et al.* 1995) permits the detection of NCX activity at $[Ca^{2+}]_i$ values (< 100 nM) at which binding of Ca^{2+} to the regulatory sites can be disregarded. Thus, in ouabain-treated D447V cells, Ca^{2+} uptake by reverse NCX

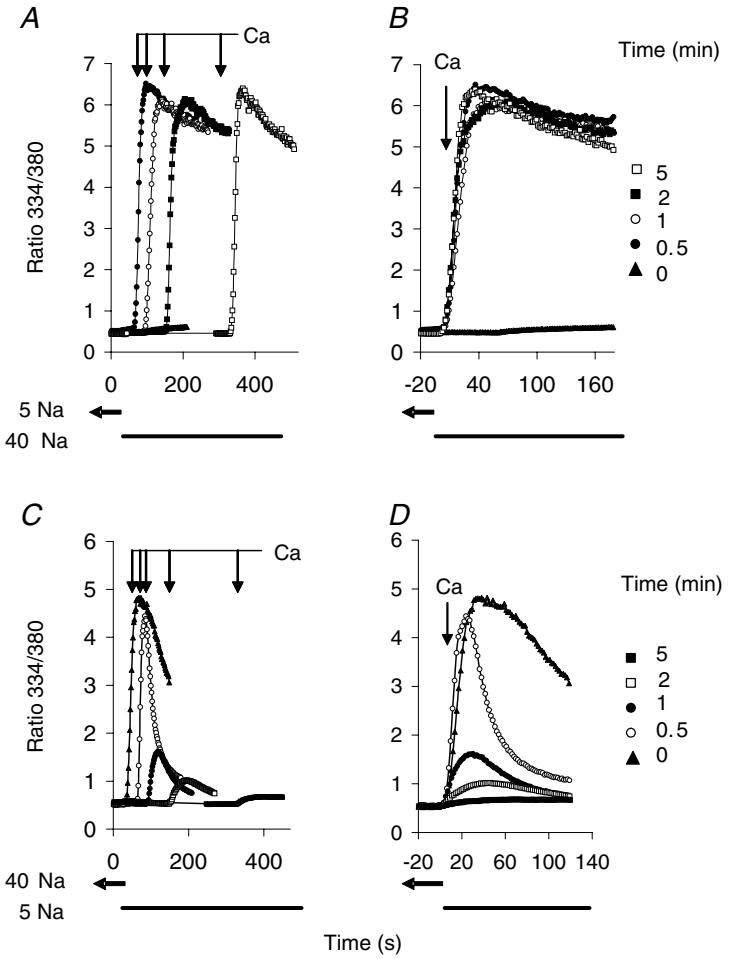

Figure 7. Time course for activation and reversibility of NCX activity
A, cells expressing the D447V mutant were treated with ATP and Tg in Na-PSS/EGTA and with gramicidin (1 μg ml^{-1}) in 5/140 Na/K-PSS 10 and 8 min, respectively, before beginning recordings. At $t = 30$ s in the figure, 4 ml of 40/100 Na/K-PSS was applied, and Ca^{2+} uptake was initiated 0.5, 1, 2 or 5 min later by applying 0.1 mM $CaCl_2$ in 40/100 Na/K-PSS. Also shown is a control trace for Ca^{2+} uptake in 5/140 Na/K-PSS initiated at 30 s without exposure to 40/100 Na/K-PSS (▲, labelled '0' in *B*). *B*, traces in *A* are superimposed; $t = 0$ in the figure refers to the time at which NCX activity was initiated. *C*, cells expressing the D447V mutant were treated with ATP and Tg in Na-PSS/EGTA and with gramicidin (1 μg ml^{-1}) in 40/100 Na/K-PSS at 10 and 8 min, respectively, before beginning recordings. At $t = 30$ s in the figure, 5 ml of 5/140 Na/K-PSS/EGTA was applied, and Ca^{2+} uptake was measured 0.5, 1, 2 and 5 min later in 5/140 Na/K-PSS. Also shown is a control trace (▲, labelled '0' in *D*) of Ca^{2+} uptake in 40/100 Na/K-PSS initiated at 30 s without exposure to 5/140 Na/K PSS. *D*, traces in *A* are superimposed; $t = 0$ refers to the time of initiation of Ca^{2+} uptake. All traces show the average response of > 50 cells from single coverslips.

activity begins without hesitation at an initial $[Ca^{2+}]_i$ of 25 nM (Fig. 2). Barium uptake is induced at similarly low values of $[Ca^{2+}]_i$ when $[Na^+]_i$ is increased to 40 mM or more (Fig. 3*A*). The absence of a lag phase for Ca^{2+} uptake by cells expressing D447V (Figs 2–4) closely mimics the behaviour of the constitutive Δ(241–680) mutant (Fig. 4). In cells expressing the wild-type NCX1.1, increasing concentrations of cytosolic Na^+ lead to a progressive shortening of the lag phase for Ca^{2+} uptake (Fig. 3*C*). This probably reflects the increasing constitutive NCX activity at elevated $[Na^+]_i$, thereby increasing the rate of Ca^{2+} uptake at very low $[Ca^{2+}]_i$ and shortening the duration of the lag period.

The possibility that elevated $[Na^+]$ could somehow induce a local submembrane $[Ca^{2+}]$ gradient that could activate D447V allosterically is not credible. Since internal Ca^{2+} stores were depleted with ATP and Tg before the commencement of our experiments, any submembrane Ca^{2+} gradient must be generated by Ca^{2+} entry from the exterior. Such a gradient might be generated during reverse-mode NCX activity, but if the submembrane Ca^{2+} were high enough to activate the D447V mutant ($K_h > 1.8\ \mu$M), it would fully activate the wild-type exchanger ($K_h \sim 0.3\ \mu$M). This possibility is ruled out by the experiment at 20 mM Na^+ with cells expressing the wild-type NCX (Fig. 4*B*), which display lag phase durations of 38 ± 24 s. The lag phases are a hallmark of incomplete allosteric Ca^{2+} activation of the exchanger, implying that initially the local Ca^{2+} concentration sensed by the exchanger in these experiments must be less than the K_h of the wild-type exchanger (300 nM), i.e. far below the level needed to activate D447V. The experiments on Ba^{2+} uptake in Fig. 3*A* also argue against the local gradient hypothesis. Submembrane Ba^{2+} gradients could conceivably be generated during Ba^{2+} entry, but Ba^{2+} is a poor allosteric activator of NCX activity, with a K_h of 10 μM for the wild-type exchanger (Trac *et al.* 1997). The K_h for Ba^{2+} activation of the D447V mutant is unknown but would be expected to be very much higher than 10 μM. The possibility that such high local concentrations of submembrane Ba^{2+} could be generated during reverse-mode activity seems extremely remote. We conclude that local submembrane Ca^{2+} or Ba^{2+} gradients, if they exist, would not be of sufficient magnitude to activate the D447V mutant in our experiments.

Our findings appear to be at variance with the well-established requirement for allosteric Ca^{2+} activation at elevated Na^+ concentrations (100 mM) in excised patches. Moreover, in excised patches, elevated Na^+ concentrations induce a time-dependent inactivation of the exchanger (I_1 inactivation) that is counteracted by high cytosolic Ca^{2+} concentrations (Hilgemann *et al.* 1992) or by PIP2 (Hilgemann & Ball, 1996). The data presented in Figs 5 and 6 suggest that the difference between our results and those obtained in excised patches may be related to the high levels of ATP and PIP2 in the intact CHO cells. Activation of PLC by the sustained elevation of $[Ca^{2+}]_i$ led to a decline in PIP2 (Fig. 6) and a profound inhibition of NCX activity in the D447V cells when they were tested shortly after $[Ca^{2+}]_i$ returned to baseline levels (Fig. 5*A* and *B*). At this time, PIP2 levels had been partly restored (Fig. 6), although NCX activity remained profoundly inhibited (Fig. 5*B*). This might indicate that high levels of PIP2 are required to elicit NCX activity under these conditions. Alternatively, when PIP2 levels are low, it seems likely that elevated $[Na^+]_i$ would induce Na^+-dependent inactivation rather than constitutive activity, and recovery from this inactivated state might be a time-dependent process, lagging behind the restoration of PIP2. In any event, NCX activity in the D447V cells was restored after several minutes at low $[Ca^{2+}]_i$ (Fig. 5*B*). We conclude that PIP2 is required for the constitutive mode of NCX activity at elevated cytosolic Na^+ concentrations.

In contrast to the D447V mutant, the Δ(241–680) mutant was not inhibited when PIP2 levels were reduced (Fig. 5*C*). This behaviour is consistent with the resistance to Na^+-dependent inactivation of this mutant (Matsuoka *et al.* 1993). The wild-type cells (Fig. 5*D*) behaved similarly to the Δ(241–680) cells, i.e. no inhibition of NCX activity was observed following PIP2 depletion. While this may seem surprising, it is probably a manifestation of persistent Ca^{2+} activation. As discussed in a previous publication (Reeves & Condrescu, 2003), when the wild-type NCX is allosterically activated by Ca^{2+}, the activated state is maintained for several tens of seconds following the return of cytosolic Ca^{2+} to low levels. Elevated Ca^{2+} is known to counteract Na^+-dependent inactivation (Hilgemann *et al.* 1992), and we conclude that the persistently activated state is similarly resistant to Na^+-dependent inactivation induced by low PIP2. This interpretation implies that in the D447V mutant, the partial activation observed at high cytosolic Ca^{2+} (Fig. 1) does not persist when $[Ca^{2+}]_i$ is subsequently reduced. Indeed, we could not demonstrate persistent Ca^{2+} activation in the D447V mutant under any conditions (data not shown). It seems likely that the low affinity of the Ca^{2+} regulatory sites in this mutant leads to a rapid decay of the activated state when $[Ca^{2+}]_i$ is reduced.

Although most excised patch data show a clear requirement for allosteric Ca^{2+} activation at elevated Na^+ concentrations, constitutive exchange activity has been observed on several occasions. Thus, in the absence of cytosolic Ca^{2+}, patches from mouse myocytes show outward exchange currents with an amplitude of ∼15% of the Ca^{2+}-activated currents in the absence of ATP; following ATP addition, which stimulates PIP2 synthesis in the excised patches (Hilgemann & Ball, 1996), mouse exchange currents become essentially independent of regulatory Ca^{2+} (Collins *et al.* 1992). Weber *et al.* (2001) also reported that mouse myocytes

often exhibit Ca^{2+}-independent outward NCX currents. The explanation for the mouse data is unclear, although it might reflect an intrinsically low rate of PIP2 hydrolysis, since the effects of transiently applied ATP in excised mouse myocyte patches do not decay for more than 30 min after ATP removal (Collins *et al.* 1992). In patches containing the guinea-pig NCX1.1, application of ATP greatly slows the rate of current decay following removal of cytosolic Ca^{2+} (Hilgemann *et al.* 1992). Patches expressing an NCX mutant (K229Q) with a high affinity for PIP2 show a large fraction of the outward exchange current that is unaffected by the removal of cytosolic Ca^{2+} (He *et al.* 2000). D. W. Hilgemann and colleagues (personal communication) have shown that outward exchange currents are unaffected by removal of Ca^{2+} after PIP2 is applied to patches from BHK cells expressing NCX1. In each of these observations, Ca^{2+}-independent NCX currents are associated with conditions that increase the amount of PIP2 in the patches; these observations support our conclusion that high levels of PIP2 are essential for the constitutive mode of NCX activity.

Our results suggest that the constitutive mode of exchange activity is induced at high cytosolic Na^+ concentrations and is absent or greatly reduced at lower $[Na^+]_i$. The underlying mechanism is unclear, but we speculate that binding of Na^+ to the translocation sites of the exchanger might induce changes in the conformational state of NCX that result in constitutive activity when PIP2 levels are high. Related conformational transitions would occur when PIP2 levels are low, but would lead instead to an inactive state, as in the classical picture of Na^+-dependent inactivation (Hilgemann *et al.* 1992). Another possible interpretation is that Na^+ itself can bind to the allosteric Ca^{2+} activation sites and stimulate activity in the absence of Ca^{2+} binding. This seems highly unlikely, however, since the D447V mutation would be likely to disrupt the putative interactions of Na^+, as well as Ca^{2+}, with the activation sites. Finally, it is also conceivable that the activity of the D447V mutant might reflect the activity of a subpopulation of exchangers that operates constitutively because the hydrophilic domain has been degraded in some way (e.g. through proteolysis). This again seems unlikely because the rates of Ca^{2+} uptake by the D447V cells are 50–60% of the maximal rates for the wild-type cells, and the putative constitutive subpopulation would then be expected to display far greater forward-mode (Ca^{2+} efflux) activity than we observed in Fig. 1.

What are the physiological implications of the results reported here? One important outcome is to counteract the prevailing notion that increases in cytosolic Na^+ inevitably lead to a downregulation of NCX activity through Na^+-dependent inactivation. This inactivating mechanism is probably a protective device to prevent NCX-mediated Ca^{2+} overload when ATP and PIP2 levels fall, as in cardiac ischaemia. Our results suggest that under normal conditions, i.e. when ATP and PIP2 levels are high, increased cytosolic Na^+ upregulates NCX activity. In normally functioning cardiac myocytes, contractile force increases sharply with $[Na^+]_i$ (Eisner *et al.* 1984; Wang *et al.* 1988; Harrison *et al.* 1992). Elevated $[Na^+]_i$ reduces the reversal potential for NCX activity ($E_{Na\text{-}Ca}$) and promotes Ca^{2+} retention by the myocardial cell, increasing the Ca^{2+} load in the sarcoplasmic reticulum and the force of contraction. The reversal potential for NCX activity becomes more negative as $[Na^+]_i$ increases and $[Ca^{2+}]_i$ decreases. By inducing constitutive activity, an increase in $[Na^+]_i$ would promote NCX activity at low $[Ca^{2+}]_i$ and would facilitate Ca^{2+} influx when the membrane potential exceeds $E_{Na\text{-}Ca}$, e.g. during the upstroke of the action potential. Increases in $[Na^+]_i$ could also promote Ca^{2+} entry during diastole. For a diastolic membrane potential of -80 mV, with ionized $[Ca^{2+}]_o = 1.25$ mM, $[Ca^{2+}]_i = 0.1\ \mu$M and $[Na^+]_o = 140$ mM, diastolic Ca^{2+} influx would occur when $[Na^+]_i \geq 17$ mM. Thus, the progressive enhancement of constitutive activity as $[Na^+]_i$ increases would progressively facilitate NCX-mediated Ca^{2+} entry at low $[Ca^{2+}]_i$ and in this way contribute to the exquisite sensitivity of contractile force to changes in $[Na^+]_i$.

References

Aharonovitz O, Zaun HC, Balla T, York JD, Orlowski J & Grinstein S (2000). Intracellular pH regulation by Na^+/H^+ exchange requires phosphatidylinositol 4,5-bisphosphate. *J Cell Biol* **150**, 213–224.

Balla T (2006). Phosphoinositide-derived messengers in endocrine signaling. *J Endocrinol* **188**, 135–153.

Blaustein MP & Lederer WJ (1999). Sodium/calcium exchange: its physiological implications. *Physiol Rev* **79**, 763–854.

Chernysh O, Condrescu M & Reeves JP (2004). Calcium-dependent regulation of calcium efflux by the cardiac sodium/calcium exchanger. *Am J Physiol Cell Physiol* **287**, C797–C806.

Collins A, Somlyo AV & Hilgemann DW (1992). The giant cardiac membrane patch method: stimulation of outward Na^+–Ca^{2+} exchange current by MgATP. *J Physiol* **454**, 27–57.

Condrescu M, Chernaya G, Kalaria V & Reeves JP (1997). Barium influx mediated by the cardiac sodium-calcium exchanger in transfected Chinese hamster ovary cells. *J Gen Physiol* **109**, 41–51.

Condrescu M & Reeves JP (2006). Actin-dependent regulation of the cardiac Na^+/Ca^{2+} exchanger. *Am J Physiol Cell Physiol* **290**, C691–C701.

DiPolo R (1979). Calcium influx in internally dialyzed squid giant axons. *J Gen Physiol* **73**, 91–113.

Eisner DA, Lederer WJ & Vaughan-Jones RD (1984). The quantitative relationship between twitch tension and intracellular sodium activity in sheep cardiac Purkinje fibres. *J Physiol* **355**, 251–266.

Fang Y, Condrescu M & Reeves JP (1998). Regulation of Na^+/Ca^{2+} exchange activity by cytosolic Ca^{2+} in transfected Chinese hamster ovary cells. *Am J Physiol* **275**, C50–C55.

Grynkiewicz G, Poenie M & Tsien RY (1985). A new generation of Ca^{2+} indicators with greatly improved fluorescence properties. *J Biol Chem* **260**, 3440–3450.

Harrison SM, McCall E & Boyett MR (1992). The relationship between contraction and intracellular sodium in rat and guinea-pig ventricular myocytes. *J Physiol* **449**, 517–550.

He Z, Feng S, Tong Q, Hilgemann DW & Philipson KD (2000). Interaction of PIP_2 with the XIP region of the cardiac Na/Ca exchanger. *Am J Physiol Cell Physiol* **278**, C661–C666.

Hilgemann DW & Ball R (1996). Regulation of cardiac Na^+,Ca^{2+} exchange and KATP potassium channels by PIP2. *Science* **273**, 956–959.

Hilgemann DW, Collins A & Matsuoka S (1992). Steady-state and dynamic properties of cardiac sodium-calcium exchange. Secondary modulation by cytoplasmic calcium and ATP. *J Gen Physiol* **100**, 933–961.

Iwamoto T, Wakabayashi S, Imagawa T & Shigekawa M (1998). Na^+/Ca^{2+} exchanger overexpression impairs calcium signaling in fibroblasts: inhibition of the $[Ca^{2+}]$ increase at the cell periphery and retardation of cell adhesion. *Eur J Cell Biol* **76**, 228–236.

Langille SE, Patki V, Klarlund JK, Buxton JM, Holik JJ, Chawla A, Corvera S & Czech MP (1999). ADP-ribosylation factor 6 as a target of guanine nucleotide exchange factor GRP1. *J Biol Chem* **274**, 27099–27104.

Levitsky DO, Nicoll DA & Philipson KD (1994). Identification of the high affinity Ca^{2+}-binding domain of the cardiac Na^+-Ca^{2+} exchanger. *J Biol Chem* **269**, 22847–22852.

Lytton J, Westlin M & Hanley MR (1991). Thapsigargin inhibits the sarcoplasmic or endoplasmic reticulum Ca-ATPase family of calcium pumps. *J Biol Chem* **266**, 17067–17071.

Matsuoka S, Nicoll DA, He Z & Philipson KD (1997). Regulation of cardiac Na^+-Ca^{2+} exchanger by the endogenous XIP region. *J Gen Physiol* **109**, 273–286.

Matsuoka S, Nicoll DA, Hryshko LV, Levitsky DO, Weiss JN & Philipson KD (1995). Regulation of the cardiac Na^+-Ca^{2+} exchanger by Ca^{2+}. Mutational analysis of the Ca^{2+}-binding domain. *J Gen Physiol* **105**, 403–420.

Matsuoka S, Nicoll DA, Reilly RF, Hilgemann DW & Philipson KD (1993). Initial localization of regulatory regions of the cardiac sarcolemmal Na^+-Ca^{2+} exchanger. *Proc Natl Acad Sci USA* **90**, 3870–3874.

Miura Y & Kimura J (1989). Sodium-calcium exchange current. Dependence on internal Ca and Na and competitive binding of external Na and Ca. *J Gen Physiol* **93**, 1129–1145.

Noda M, Shepherd RN & Gadsby DC (1988). Activation by $[Ca^{2+}]_i$, and block by 3′,4′-dichlorobenzamil, of outward Na/Ca exchange current in guinea-pig ventricular myocytes. *Biophys J* **53**, 342a.

Opuni K & Reeves JP (2000). Feedback inhibition of sodium/calcium exchange by mitochondrial calcium accumulation. *J Biol Chem* **275**, 21549–21554.

Ottolia M, Philipson KD & John S (2004). Conformational changes of the Ca^{2+} regulatory site of the Na^+-Ca^{2+} exchanger detected by FRET. *Biophys J* **87**, 899–906.

Reeves JP & Condrescu M (2003). Allosteric activation of sodium-calcium exchange activity by calcium: persistence at low calcium concentrations. *J Gen Physiol* **122**, 621–639.

Rhee SG (2001). Regulation of phosphoinositide-specific phospholipase C. *Annu Rev Biochem* **70**, 281–312.

Trac M, Dyck C, Hnatowich M, Omelchenko A & Hryshko LV (1997). Transport and regulation of the cardiac Na^+-Ca^{2+} exchanger, NCX1. Comparison between Ca^{2+} and Ba^{2+}. *J Genl Physiol* **109**, 361–369.

Várnai P, Lin X, Lee SB, Tuymetova G, Bondeva T, Spat A, Rhee SG, Hajnoczky G & Balla T (2002). Inositol lipid binding and membrane localization of isolated pleckstrin homology (PH) domains. Studies on the PH domains of phospholipase C delta 1 and p130. *J Biol Chem* **277**, 27412–27422.

Wang DY, Chae SW, Gong QY & Lee CO (1988). Role of aiNa in positive force-frequency staircase in guinea pig papillary muscle. *Am J Physiol* **255**, C798–C807.

Weber CR, Ginsburg KS & Bers DM (2005). Allosteric regulation of cardiac Na/Ca exchange by cytosolic Ca: dynamics during $[Ca]_i$ changes in intact myocytes. *Biophys J* **88**, 136a.

Weber CR, Ginsburg KS, Philipson KD, Shannon TR & Bers DM (2001). Allosteric regulation of Na/Ca exchange current by cytosolic Ca in intact cardiac myocytes. *J Gen Physiol* **117**, 119–131.

Acknowledgements

We are grateful to Drs Deborah Nicoll and Kenneth D. Philipson for providing the cDNAs for the wild-type canine exchanger and the D447V mutant and to Drs Tamas Balla and Larry Gaspers for the gift of PLCδ1PH-GFP. Thanks also to Drs Larry Hryshko and Mark Hnatowich for conversations that led to the initiation of this project. We also gratefully acknowledge the help of Dr Donald Hilgemann for providing us with his unpublished data on the induction of constitutive activity by PIP2 in excised patches. This work was supported by NIH grant HL 49932. Jason Urbanczyk was supported by NIH training grant 1 T32 HL069752.